Jurnal Teknik Mesin
Mechanical Xplore (JTMMX)
Mechanical Engineering
Vol. 5 No. 1 (2024) pp. 13-23
p-ISSN: 2746-0045 e-ISSN: 2746-3672

Improving Dissimilar Metal Joining Quality Through Shielded Metal Arc Welding: A Taguchi Optimization Strategy

Agus Supriyanto[1], Sukarman [1*], Dodi Mulyadi[1], Nazar Fazrin[1], Apang Djafar Shieddieque[2], Khoirudin[1,3], Amri Abdulah[2,3], Otong Jaelani[4]

[1]Department of Mechanical Engineering, Faculty of Engineering, University of Buana Perjuangan Karawang, Karawang, West Java, 41313, Indonesia.
[2]Department of Mechanical Engineering, Sekolah Tinggi Teknologi Wastukancana, Purwakarta, 41151, Indonesia.
[3]Department of Mechanical Engineering, Faculty of Engineering, Universitas Sebelas Maret, Surakarta, 57126, Central Java, Indonesia.
[4]Department of Mechanical Engineering, STT Mandala, Bandung, West Java, 40284, Indonesia

ABSTRACT

The results of an experiment that used an orthogonal Taguchi method to improve shielded metal arc welding (SMAW) were given. The SMAW method was used to join dissimilar metals of SPHC and St. 30. SPHC material has a low carbon steel content, while St. 30C steels contain a medium amount of carbon steel used for tractor shaft axles. Carbon percentages vary slightly between the two substances. This study aimed to achieve the highest possible tensile strength quality by utilizing the specified SMAW parameters. SPHC material has a low carbon content, whereas St. 30 steel has a moderate carbon content. This study used the Taguchi experimental method with three input variables and three experimental levels. The SNR ratio is used to evaluate the most optimal SMAW performance. ANOVA analysis evaluates the most crucial parameters in determining the response variable. This research has successfully provided input on the combination of SPHC and St. 30C for SMEs. It operates effectively with a welding current of 133 A, a welding voltage of 9 V, and a filler diameter of 2.0 mm. The S/N ratio analysis found that the welding current, voltage, and filler diameter significantly impacted the outcome.

Keywords: *Taguchi method; Tensile strength; Dissimilar joint metal; Shielded metal arches welding; SPHC/St.30*

Article information:
Submitted: 26/\07/2024
Revised: 07/09/2024
Accepted: 08/09/2024

Author correspondence:
* ✉:
sukarman@ubpkarawang.ac.id

Type of article:
☑ Research papers
☐ Review papers

1. INTRODUCTIONS

This paper aims to optimize the tensile strength in the shielded metal arc welding (SMAW) process, with a specific focus on fusing dissimilar steels—SPHC/St. 30. The financial constraints that govern the availability of automated welding equipment pose a substantial barrier for MSMEs. To address this discrepancy, individuals often require technical guidance when joining dissimilar materials together, such as SPHC steel sheets and St. 30 steel round bars. The flux on the SMAW electrode protects the weld metal from oxygen as it melts and solidifies during the welding applications [1]. Applying welding processes and joining materials, such as tractor shafts, is essential to developing rugged products [2]. However, this process frequently consumes most of the product's cost and causes more production difficulties than anticipated [3]. Tractor shaft axles are typically made of hardened steel or other high-strength materials to withstand the heavy

loads and torque applied during operation. They are designed to be durable and resistant to bending or twisting forces. The shaft axle is located at the tractor's rear and carries most of the vehicle's weight as shows in Figure 1 [4]. It transfers power to the rear wheels and often incorporates a differential to allow the wheels to rotate at different speeds during turns Figure 1 (b) provides information on T-joint welding between the shaft and holder shaft axle. T-joint welding is a joint configuration commonly used in welding where two pieces of metal are joined together to form a T shape [5]. It is a fundamental welding joint widely used in various industries and applications. A T-joint is formed when one piece of metal is perpendicular to another, creating a T shape. The joint requires welding along the fillet where the two pieces intersect [5]. Shielded Metal Arc Welding (SMAW) is a fusion welding process that utilizes a consumable electrode coated with flux [6]. The electrode, also known as a welding rod or stick, consists of a core wire that serves as a filler metal and a flux coating that shields the weld pool from atmospheric contamination [7]. SMAW is characterized by its simplicity, versatility, and suitability for both indoor and outdoor welding. SMAW finds applications in a wide range of industries, including construction, infrastructure, maintenance and repair, pipelines, shipbuilding, automotive, and manufacturing [8].

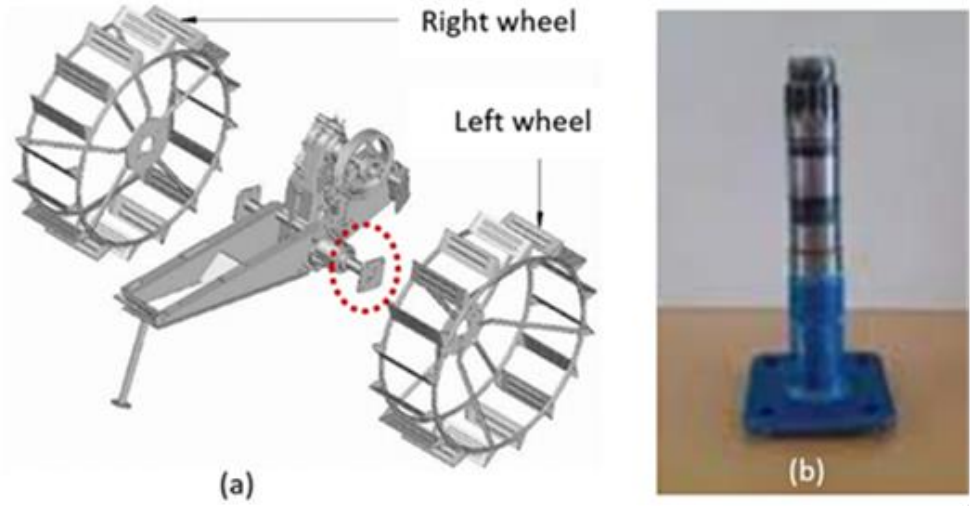

Figure 1. Illustration of Tractor quick G1000: (a) the tractor's drivetrain system, (b) Tractor shaft axles-quick G1000.

It is commonly used for structural steel fabrication, repair welding, maintenance work, and field welding in demanding environments. The following sections describe some of the SMAW welding research that has been conducted. Datta et al. conducted a SMAW study in which high-strength Q & T material quenched and tempered plates) were incorporated into the impeller manufacturing process [4]. The minimum tensile strength of SA 517 material Q & T alloy steel was 670 MPa. The shielded metal arc welding (SMAW) technique was used to evaluate the locally developed resistance of high-strength Q & T steels to cold cracking. The static fatigue limit values significantly exceed the minimum specified yield strength of 670 MPa and the critical restraint intensity (Kcr) of 34,650 MPa. The tensile strength of 812.4 MPa and impacted toughness at -40oC of the welded joints were 88.3 to 63.4 J.

The effect of SMAW welding process parameters on waveform formation was investigated by Kah et al [6]. The power source development, specifically short circuits, managed polarity, and electrode wire movement, was chosen for the SMAW input variable. The output variables selected were weldability and mechanical properties. The primary goals were to decrease heat input, eliminate harmful splashing, and increase welding process flexibility. The modified SMAW process can be beneficial for thinner sheet metal, stainless steel, and heat-sensitive steel sheet.

Karuthapandi et al. [9] investigated the relationship between welding microstructure and welding parameters in GTAW wire electrodes. Flat-wire electrodes were used to make bead-on-plate welds, and the input parameters included welding speed, welding current, and flat-wire electrode direction. The

microstructure properties of the weld zone were investigated, including deposition, reinforcement height, overall bead width, bead width, HAZ depth, and penetration depth. Flat wire electrodes increased the depth-to-width ratio (D/W) at GMAW by 16.5 % compared to when the electrodes were commonly used. A fuzzy logic model was developed using simulated data to estimate the effect of a flat electrode on weld shape characteristics. The experimental results validate the model's predictions.

Numerous studies have focused on the optimization of SMAW welding, but none have examined the optimization of SPHC (JIS G 3131) and St. 30 (JIS G 4051) steel round bars in the application. In contrast to previous SMAW optimization studies, the current investigation employs SPHC steel sheets and St. 30 steel round bars. This study utilized the Taguchi orthogonal experiment method with three experimental design levels and three parameters. The three levels are current at 90A, 110A, and 135A; voltage at 8V, 9V, and 10V; and filler diameter at 2.0 mm, 2.6 mm, and 3.0 mm. The objective of this study was to determine the optimal way to use the SMAW technique to join various metals to SPHC steel sheets and St. 30 round steel to achieve the highest tensile strength test results.

2. METHOD

2.1. Materials

This work utilized a base metal configuration of 3 mm SPHC and 12 mm St. 30 round bars. Based on recognized steel carbon content classifications, St. 30 material belongs to the medium-carbon steel category and has an approximate carbon content of 0.323% [10, 11]. A pivotal consideration in selecting the filler material is ensuring its melting point closely matches the intended base metal for fusion. It necessitates a comprehensive assessment of the carbon-based metal in the fusion process when determining the optimal melting point. The mechanical properties of SPHC and St. 30 listed in Table 1.

Table 1. The Mechanical properties of SPHC and St. 30 materials

Properties of material	**SPHC (%)**		**St. 30 (%)**	
	JIS G3131 [13]	**Specimen[1)]**	**JIS G4051 [14]**	**Specimen[2)]**
Tensile strength	≤ 0.15	0.0268	0.27 - 0.33	0.323
Yield strength	≤ 0.05	0.0192	0.15 - 0.35	0.268
Hardness	≤ 0.60	0.1980	> 0.6 - 0.9	0.710

1) Mill certificate, [2)] Test certificate

The chemical composition of the SPHC material, which complies with the JIS G3131 standard [13], is as follows: carbon (C) is a maximum of 0.15%, with an actual value of 0.0268%; silicon (Si) is a maximum of 0.05%, with an actual value of 0.0192%; manganese (Mn) is a maximum of 0.60%, with an actual value of 0.1980%; phosphorus (P) is a maximum of 0.035%, with an actual value of 0.0125%; and sulfur (S) is a maximum of 0.035%, with an actual value of 0.0141%.

The St. 30 material adheres to the JIS G4051 standard [14] and has the following chemical composition: carbon (C) ranges from 0.27-0.33%, with an actual value of 0.323%; silicon (Si) ranges from 0.15-0.35%, with an actual value of 0.268%; manganese (Mn) ranges from >0.6-0.9%, with an actual value of 1.130%; phosphorus (P) is less than 0.030%, with an actual value of 0.008%; and sulfur (S) is less than 0.035%, with an actual value of 0.009%.

The fundamental parameters in filler selection involve matching the base metal's mechanical properties and ensuring the filler's chemical composition is as close to the base metal as possible [12]. Consideration must also be given to the power supply, welding position, and joint design [8]. The AWS A5.1 E6013 filler meets these standards, with a carbon (C) content of 0.080%, well below the 0.2% limit, reducing the risk of weld cracking. Manganese (Mn) at 0.400%, below the 1.2% limit, enhances weld strength and toughness. Silicon (Si) at 0.024%, under the 0.1% limit, acts as an effective deoxidizer. Additionally, low levels of sulfur (S) and phosphorus (P)—0.014% and 0.008%, respectively—help avoid cracking and brittleness in the weld.

The AWS A5.1 E6013 filler also exhibits excellent mechanical properties. Its ultimate tensile strength (UTS) of 500 MPa exceeds the standard minimum of 444 MPa. In comparison, its yield strength (YS) of 425 MPa surpasses the minimum requirement of 331 MPa, indicating strong resistance to permanent deformation. The material demonstrates high flexibility and ductility with an elongation of 26.7%, well above the 17% minimum. These attributes confirm that AWS A5.1 E6013 is highly suitable for welding applications requiring strength and ductility.

2.2. Welding design and tensile strength test

The welding procedure employs the T-joint connection method in alignment with the specific conditions of the tractor shaft [13]. It is imperative that the T-joint welding process strictly adhere to established safety regulations and is executed by qualified welding operators. In the initial phase, the bending of SPHC steel is performed to align with the guidelines depicted in Figure 2. Subsequently, the welding operation involving SPHC and St. 30C materials follows the parameters outlined in Table 2. Finally, the concluding step entails a meticulous surface refinement process employing sandpaper, systematically progressing through grades 200, 400, 600, and 800 and concluding with 1000.

Each parameter in the test sample has been provided in two pieces for a tensile test—the welding performance test aimed to determine the parameter combination with the highest tensile strength. The Method for Tensile Testing of Metallic Materials refers to ASTM E8. It was chosen to evaluate tensile strength [14, 15]. The test specimen was pulled with a specific force and velocity controlled [16-18]. **Error! Reference s ource not found.** depicts the tensile strength test of SMAW welding coupons.

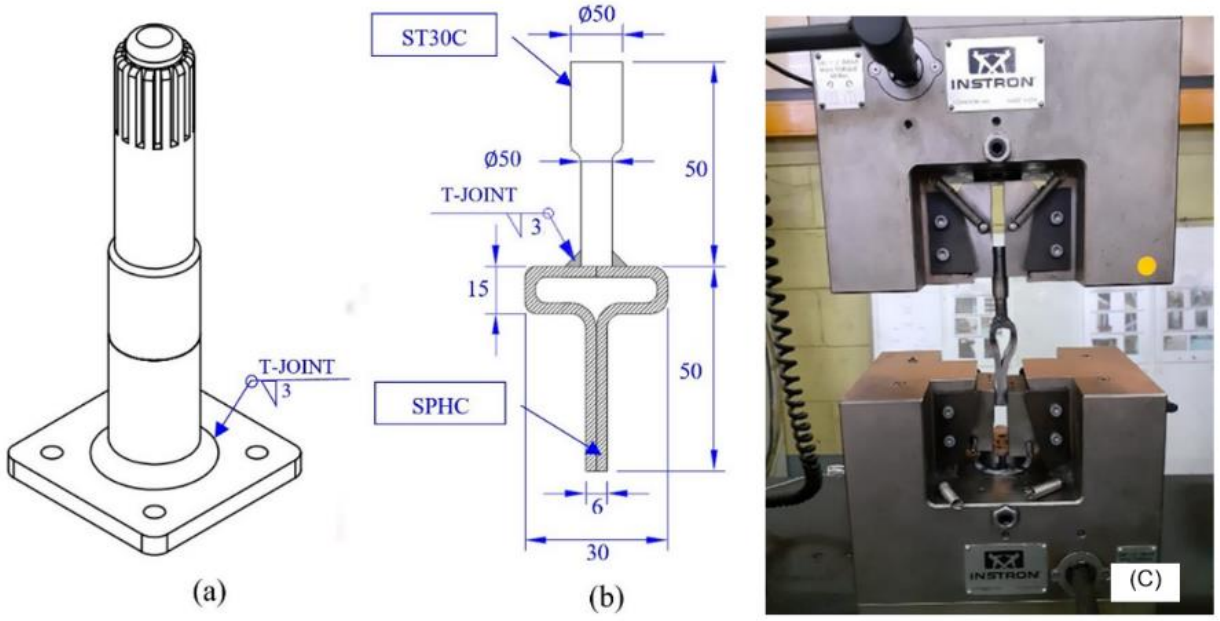

Figure 2. Illustration of Tractor quick G1000: (a) the tractor's drivetrain system, (b) Tractor shaft axles-quick G1000 [4].

2.3. Taguchi experimental design

Taguchi Orthogonal array experimental design optimized the tensile strength of the SMAW method. An orthogonal array is a matrix representing a set of experiments with varying levels of factors. It is designed so that each column represents a factor, and each row represents a combination of factor levels. The key characteristic of an orthogonal array is that it ensures an equal and balanced representation of all factor combinations [19-21]. The level of orthogonality in an orthogonal array refers to the extent to which the interactions between factors are minimized. Higher levels of orthogonality result in reduced interactions, making it easier to analyze the effects of individual factors.

This study used three parameters and a three-level experimental design. The experiment was developed to identify various input parameters, responses and corresponding levels [12]. The filler diameter, voltage, and current have been selected for input parameters. The response variable was measured to determine the tensile

strength of joining dissimilar metals, such as SPHC steel sheets and St. 30 round bars. Statistical software was used to create the Taguchi experimental orthogonal array by L9 (3^3). The highest tensile strength was tracked while each factor was chosen as a response variable. The methods used to measure the three factors and three levels are listed in Table 2.

The concept of "SNR analysis" is crucial to the Taguchi experimental design. The desired value of the output (response variable) is referred to as a "signal" [22-24]. The term "noise" refers to the undesirable value output [25, 26]. Signal-to-noise ratio (S/N ratio) is a measure used to quantify the level of signal strength compared to the level of background noise or interference in a system or signal. The quality attributes of the targeted variable response affect the SNR analysis.

Table 2. Taguchi experimental design

Code	Welding factors	Level		
		1	2	3
A	Current (A)	90	110	135
B	Voltage (V)	8	9	10
C	Filler diameter (mm)	2.0	2.6	3.0

The signal-to-noise ratio can be calculated in various ways depending on the specific context and measurement techniques. The S/N ratio in decibels is calculated using the formula 1, 2, and 3 [20, 23, 27, 28].

Smaller is better:

$$SNR = -10 \log \sum_{i=1}^{n_0} \frac{y_i^2}{n_0} \quad (1)$$

Larger is better:

$$SNR = -10 \log \frac{1}{n_0} \sum_{i=1}^{n_0} \frac{1}{y_i^2} \quad (2)$$

Nominal is the best:

$$SNR = -10 \log \frac{\bar{y}^2}{s^2} \quad (3)$$

Where n s, y, and $\bar{y}$ are the sample number, the variance of the response, response factor, and mean response factor.

The SNR with characteristic data 'larger is better' was used in this study to achieve the highest tensile strength in the SMAW welding process. The SNR of characteristic data "larger is better" was used in this study to determine the maximum tensile strength of the SMAW process. The measurable SNR characteristic "larger is better" has a non-negative value including an infinite ideal value [29]. It has been successfully implemented in industrial processing, such as resistance spot welding [30], plastic fiber [31], textile industries [32], metal forming [33], machining non-conventional [26] and controlled dry film thickness powder paint [34]. Table 3 displays the design parameters that maximize the tensile strength of shielded metal arc welding procedures.

Table 3. The design variables of the optimization experiment

Run	Welding factor			Sample codes	
	Weld. current (A)	Voltage (V)	Filler diameter (mm)	S1	S2
1	90	8	2.0	1-S1	1-S2
2	90	9	2.6	2-S1	2-S2
3	90	10	3.2	3-S1	3-S2
4	110	8	2.6	4-S1	4-S2
5	110	9	3.2	5-S1	5-S2
6	110	10	2.0	6-S1	6-S2
7	135	8	3.2	7-S1	7-S2
8	135	9	2.0	8-S1	8-S2
9	135	10	2.6	9-S1	9-S2

2.4. *Statistic confirmation*

Analysis of Variance (ANOVA) will be performed to assess the significance of each factor and their interactions on weld quality. The factors under investigation include welding current (A), voltage (V), and filler diameter (mm). ANOVA will determine which of these factors have a statistically significant impact on the welding responses and quantify their contributions. Additionally, interaction plots will be generated to visualize the interactions between these factors. These plots will illustrate how the effect of one factor varies at different levels of another factor, providing valuable insights into the complex interactions within the welding process.

3. RESULTS AND DISCUSSION

3.1. *Tensile strength performance analysis*

A tensile strength test was conducted to evaluate the performance of coupon welding. The analysis of various combinations of SMAW welding parameters aimed to identify which variable most significantly affects the response variable. The highest tensile strength measured was 481.74 MPa, obtained from the first sample coupon of the seventh experiment, as shown in Figure 3. This sample used a welding current of 135 amps, a voltage of 8 volts, and a filler diameter of 3.2 mm. In contrast, the lowest tensile strength was 232.20 MPa, observed in the first sample coupon from the fifth experiment, which had a welding current of 110 amps, a voltage of 9 volts, and a filler diameter of 2.6 mm.

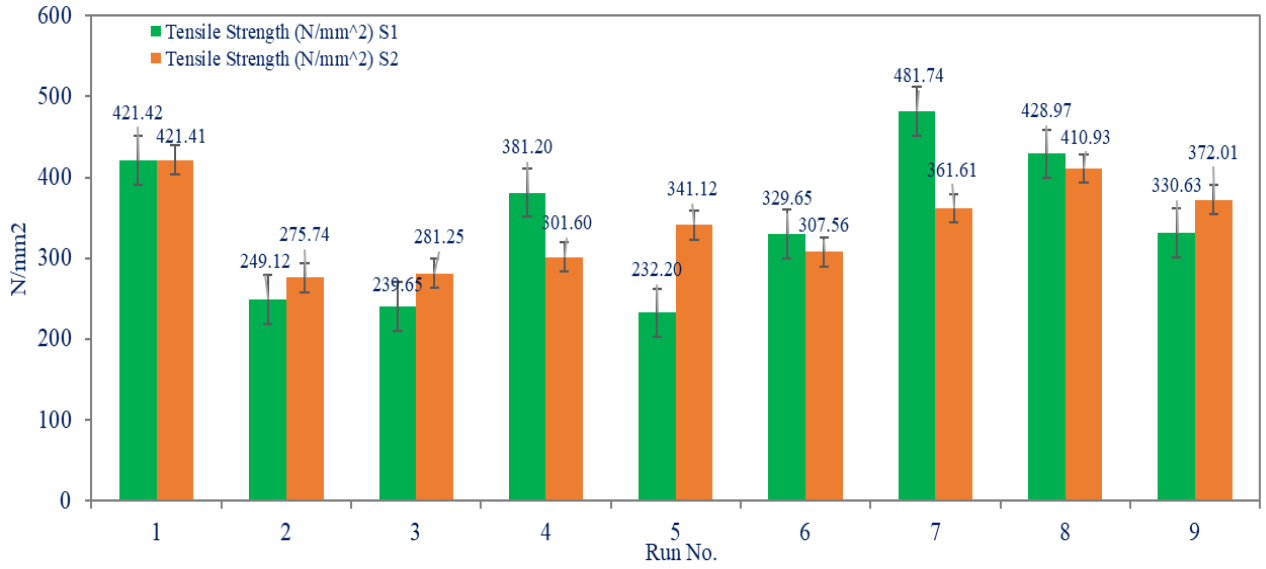

Figure 3. Tensile strength test result of each coupon

3.2. *Signal-to-noise ratio (SNR) analysis*

Orthogonal arrays (OAs) were utilized to assign sample groups precisely. The OA matrix facilitates the accurate assignment of standard specifications to efficiently produced test groups and is characterized by critical factors [27]. In empirical studies, practical levels are often used. For this investigation, three levels of experimentation were applied for each significant factor. The study employed the L9 (3^2) array, contrasting with the OA used. This array considered three-level control parameters, resulting in six degrees of freedom. The selected L9 OA with 8 degrees of freedom (DOF) is shown in Table 4. Linear regression models for the mean tensile strength signal-to-noise ratio (SNR) were developed using statistical software [35, 36]. The predictors in these models include welding current (amps), welding voltage (volts), and welding filler metal diameter (mm). Using a Taguchi experimental design, the output is modelled using the response. Equation 4 represents the SNR corresponding to the linear regression model.

$$SNR_{Pred.} = 53.99 + 0.0496\,A - 1.011B \quad (4)$$

Table 4. The SNR with 'Larger is better' characteristic data

Level	A	B	C
1	49.69	51.74	51.67
2	49.74	49.83	49.90
3	51.85	49.72	49.71
Delta	2.16	2.02	1.95
Rank	1	2	3

The Taguchi experimental method evaluates the degree of responsiveness of a given characteristic to variable inputs in a controlled development process, using a metric called the 'signal-to-noise ratio' (SNR) [30] . SNR analysis seeks to determine the optimal levels of various inputs that result in the best response. For the required responses, the Taguchi design proposes that the optimal condition can be achieved by adjusting each input factor of the output characteristic [25]. Based on this method, the best tensile strength test was performed with the welding current set at the third level, voltage set at the first level, and filling at the first level. Figure 4 illustrates the optimal SMAW parameters suggested by the Taguchi design.

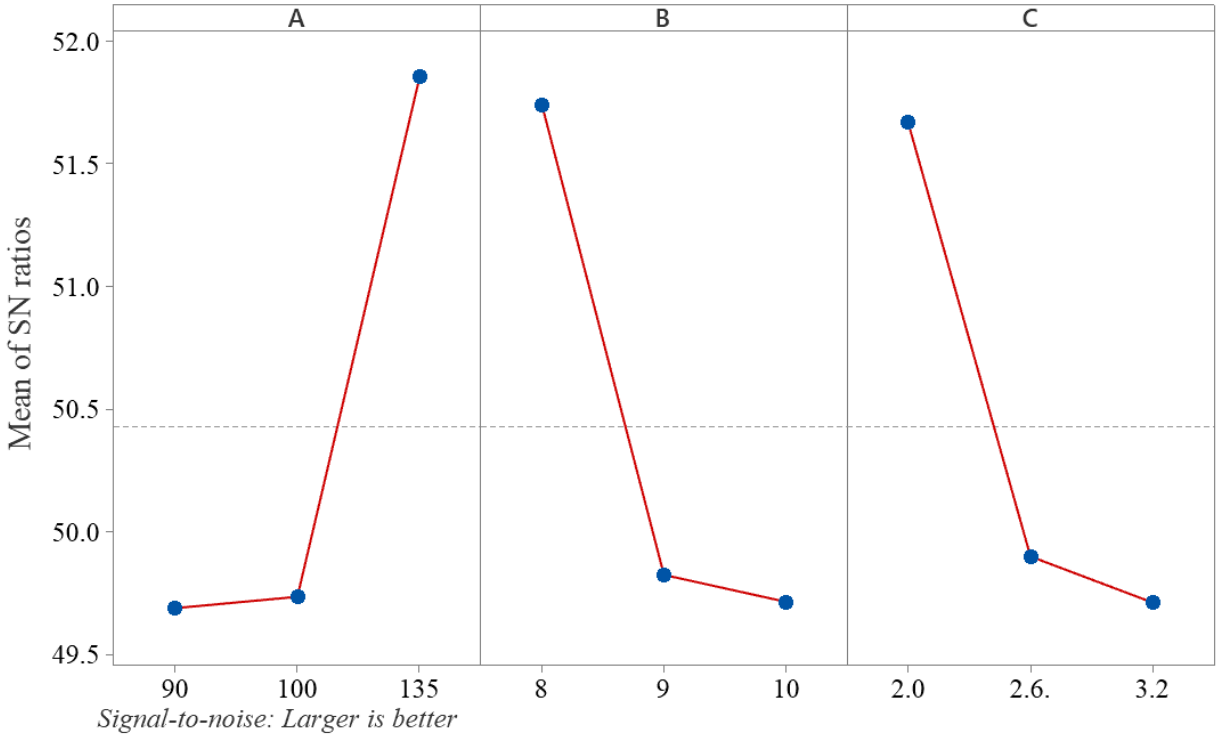

Figure 4. Main effects plot of the 'larger is better' signal-to-noise ratio (SNR) for the SMAW method.

The value of the signal-to-noise ratio (SNR) was directly proportional to the average tensile strength of the SMAW welding current. Since the SNR uses the "larger is better" criterion, the third level of welding current produced the greatest response effect, in comparison to the first and second experimental levels. The variables of voltage and filler diameter exhibited an inverse proportionality to the response variable of tensile strength. This experiment demonstrated a direct relationship between an increase in both voltage and filler diameter parameters and a decrease in tensile strength. Table 5 provides the results of the SNR analysis of the SMAW parameters.

The variable input that significantly influences the variable output (tensile strength) when incorporating SPHC and ST. 30C is welding current, with a delta value of 2.16, followed by welding voltage and filler diameter, each with a delta value of 1.92. Table 5 presents the response table for the SNR for each SMAW method input parameter.

Table 5. Tensile strength of SMAW welding and SNR experimental data

RUN No.	Weld current (A)	Voltage (V)	Filler Dia. (mm)	Tensile Strength (N/mm^2)			*SNR*	
				S-1	S-2	Mean	Exp.*)	Pr.**)
1	90	8	2.0	421.42	421.41	421.4	52.49	50.37
2	90	9	2,6	249.12	275.74	262.4	48.35	49.36
3	90	10	3,2	239.65	281.25	260.5	48.23	48.34
4	110	8	2,6	381.20	301.60	309.9	50.49	51.36
5	110	9	3,2	232.20	341.12	286.7	48.67	50.35
6	110	10	2.0	329.65	307.56	318.6	50.05	49.34
7	135	8	3,2	481.74	361.61	421.7	52.23	52.60
8	135	9	2.0	428.97	410.93	424.5	52.46	51.59
9	135	10	2,6	330.63	372.01	346.3	50.87	50.58

* Experimental, ** Predicted

3.3. Statistical analysis

ANOVA was employed to assess the statistical significance of each constrained parameter's effect on response factors. This technique quantifies the contribution of each factor by comparing the total squared values of the control variables across all process parameters. Table 6 presents the ANOVA results for the SMAW method. The analysis reveals that welding current and voltage significantly impact the tensile strength of SMAW welds, as indicated by P-values below 5%. In contrast, the filler diameter minimises tensile strength, with a P-value more significant than 5% (P > 5%). The percentage contribution analysis shows that welding current and voltage account for approximately 75% of the variance in tensile strength, while the filler diameter contributes about 25%. These findings corroborate the results of Vimal et al., who identified welding current and voltage as the most influential factors on the tensile strength of SMAW-welded materials [8].

Table 6. The ANOVA for tensile strength measures

Source	DF	Seq. SS	Adj. MS	P-value	Contribution
Weld current (A)	2	13609.6	6804.8	0.039	39%
Voltage (V)	2	12498.7	6249.3	0.042	36%
Filler Dia. (mm)	2	8743.2	4371.6	0.060	25%
Residual Error	2	554.6	277.3		
Total	8	35406.0			100%

The interaction plot illustrates the relationship between one input factor and the continuous response, which varies depending on the value of a second input factor. In this diagram, the x-axis represents the averages for one-factor level, while separate lines are plotted for each level of the other factor. Parallel lines in the interaction plot suggest no interaction between factors, whereas non-parallel lines indicate an interaction. The greater the deviation from parallelism, the stronger the interaction effect [25, 26]. Figure 5 shows the interaction plots for welding current (A) vs voltage (B), welding current (A) vs filler diameter (C), and voltage (B) vs filler diameter (C). The analysis reveals that the interaction between the first and second input variables significantly affects tensile strength as the response variable in this study.

4. CONCLUSIONS

A tensile strength test evaluated coupon welding performance using various SMAW parameter combinations. The highest tensile strength recorded was 481.74 MPa, achieved with a welding current of 135 amps, a voltage of 8 volts, and a filler diameter of 3.2 mm. Conversely, the lowest tensile strength of 232.20 MPa was noted with a welding current of 110 amps, a voltage of 9 volts, and a filler diameter of 2.6 mm. The experimental results indicated that welding current, voltage, and filler diameter significantly affected the tensile strength, with delta values of 2.16, 2.02, and 1.95, respectively. The highest average tensile strength of 424.5 MPa was achieved in the eighth iteration with 135 amps, 9 volts, and a filler diameter of 2 mm. ANOVA

analysis revealed that welding current is the most critical variable, followed by voltage and filler diameter. The interaction plot illustrated how one input factor influences a continuous response based on the value of a second input factor, with parallel lines indicating no interaction and non-parallel lines suggesting interaction. These findings are relevant for welding processes in small and medium industries. Future research will focus on other material specifications, particularly the SMAW SPHC and St.30 welding processes.

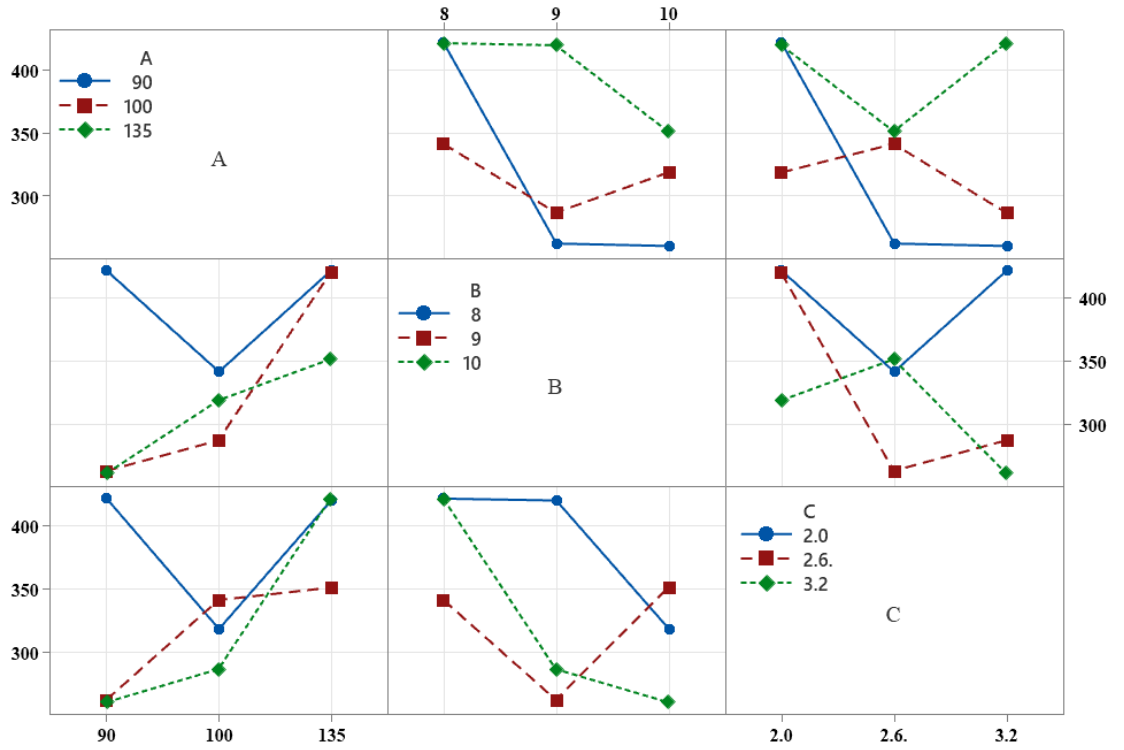

Figure 5. The interaction plot of SMAW parameters

AUTHOR'S DECLARATION

Authors' contributions and responsibilities

The authors made substantial contributions to the conception and design of the study. The authors took responsibility for data analysis, interpretation and discussion of results. The authors read and approved the final manuscript.

Acknowledgment

This research was funded by a grant from the University of Buana Perjuangan Karawang, STT Wastukancana Purwakarta, and STT Mandala Bandung, West Java. Special thanks to PT Gama Engineering for providing the workshop facilities to prepare the samples.

Availability of data and materials

All data are available from the authors.

Competing interests

The authors declare no competing interest

REFERENCES

[1] B. Anwar, "Analisis Kekuatan Tarik Hasil Pengelasan Tungsten Inert Gas (Tig) Kampuh V Ganda Pada Baja Karbon Rendah St 37," *Teknologi*, vol. 17, no. 3, pp. 33-38, 2018.

[2] J. Lancaster, *Handbook of structural welding* (Hanbook of structural welding Processes, materials and methods used in the welding pf major structures, pipeline and process plant). England: Abington Publishing, 1997.
[3] D. L. Olson, S. Thomas A, S. Liu, and G. R. Edwards, *Welding, brazing, and soldering*. ASM International, 1990.
[4] R. Datta, D. Mukerjee, S. Jha, K. Narasimhan, and R. Veeraraghavan, "Weldability characteristics of shielded metal arc welded high strength quenched and tempered plates," *Journal of Materials Engineering and Performance*, vol. 11, no. 1, pp. 5-10, 2002.
[5] J. P. Oliveira, K. Ponder, E. Brizes, T. Abke, A. J. Ramirez, and P. Edwards, "Combining resistance spot welding and friction element welding for dissimilar joining of aluminum to high strength steels," *Journal of Materials Processing Technology*, vol. 273, no. January, pp. 116192-116192, 2019.
[6] P. Kah, R. Suoranta, and J. Martikainen, "Advanced gas metal arc welding processes," *International Journal of Advanced Manufacturing Technology*, vol. 67, no. 1-4, pp. 655-674, 2013.
[7] *Boiler & Pressure Vessel Code II Part D Properties (Matrix) Materials*, 978-07918-3235-6, 2010.
[8] K. E. K. Vimal, S. Vinodh, and A. Raja, "Optimization of process parameters of SMAW process using NN-FGRA from the sustainability view point," *Journal of Intelligent Manufacturing*, vol. 28, no. 6, pp. 1459-1480, 2017.
[9] S. Karuthapandi, M. Ramu, and P. R. Thyla, "Effects of the use of a flat wire electrode in gas metal arc welding and fuzzy logic model for the prediction of weldment shape profile," *Journal of Mechanical Science and Technology*, vol. 31, no. 5, pp. 2477-2486, 2017.
[10] A. A. M. Aws, "AWSA5.18-A5.18M-2005.pdf," ed, 2005.
[11] A. Abdurahman, S. Sukarman, A. Djafar Shieddieque, S. Safril, D. Setiawan, and N. Rahdiana, "EVALUASI KEKUATAN UJI TARIK PADA PROSES PENGELASAN BUSUR LISTRIK BEDA MATERIAL SPHC DAN S30-C," *Jurnal Teknik Mesin Mechanical Xplore*, vol. 1, no. 2, pp. 29-37, 2021.
[12] G. E. Linneert, *WELDING METALLURGY*, 4 ed. American Welding Society, 1994.
[13] Asme, "ASME Boiler and Pressure Vessel Code, Section II Part C - Specifications for Welding Rods, Electrodes, and Filler Metals,"Specification for titanium and titanium-alloy welding electrodes and rods"," ed, 2010, pp. 377-390.
[14] *Hot-rolled mild steel plates, sheet and strip*, 2010.
[15] *ASTM E8/E8M Standard Test Methods for Tension Testing of Metallic Materials*, 2013.
[16] S. Sukarman *et al.*, "OPTIMAL TENSILE-SHEAR STRENGTH OF GALVANIZED/MILD STEEL (SPCC-SD) DISSIMILAR RESISTANCE SPOT WELDING USING TAGUCHI DOE," *Jurnal Teknologi*, vol. 4, pp. 167-177, 2023.
[17] K. Khoirudin, S. Sukarman, N. Rahdiana, and A. Fauzi, "ANALISIS FENOMENA SPRING-BACK / SPRING-GO FACTOR PADA LEMBARAN BAJA KARBON RENDAH MENGGUNAKAN PENDEKATAN EKSPERIMENTAL," *Jurnal Teknologi*, vol. 14, no. 1, 2022.
[18] F. Mucharom *et al.*, "Tensile shear load in resistance spot welding of dissimilar metals: An optimization study using response surface methodology," *Mechanical Engineering for Society and Industry*, vol. 3, no. 2, pp. 66-77, 2023.
[19] S. B. Sutono, "Grey-based Taguchi Method to Optimize the Multi-response Design of Product Form Design," *Jurnal Optimasi Sistem Industri*, vol. 20, no. 2, pp. 136-146, 2021.
[20] S. Sukarman, A. Abdulah, A. D. Shieddieque, N. Rahdiana, and K. Khoirudin, "OPTIMIZATION OF THE RESISTANCE SPOT WELDING PROCESS OF SECC-AF AND SGCC GALVANIZED STEEL SHEET USING THE TAGUCHI METHOD," *SINERGI*, vol. 25, no. 3, pp. 319-328, 2021.
[21] S. Shafee, B. B. Naik, and K. Sammaiah, "Resistance Spot Weld Quality Characteristics Improvement By Taguchi Method," *Materials Today: Proceedings*, vol. 2, no. 4-5, pp. 2595-2604, 2015.
[22] A. Abdulah, S. Sukarman, C. Anwar, A. Djafar Shieddieque, and A. Ilmar Ramadhan, "Optimization

of yarn texturing process DTY-150D/96F using taguchi method," *Technology Report of Kansai University*, vol. 62, no. 4, pp. 1471-1479, 2020.
[23] A. G. Thakur and V. M. Nandedkar, "Optimization of the Resistance Spot Welding Process of Galvanized Steel Sheet Using the Taguchi Method," *Arabian Journal for Science and Engineering*, vol. 39, no. 2, pp. 1171-1176, 2014.
[24] P. Muthu, "Optimization of the Process Parameters of Resistance Spot Welding of AISI 316l Sheets Using Taguchi Method," *Mechanics and Mechanical Engineering*, vol. 23, no. 1, pp. 64-69, 2019.
[25] P. G. Mathews, *Design of Experiments with MINITAB*, 12 ed. Milwaukee: Mathews, Paul G., 2005, pp. 205-205.
[26] S. Chandramouli and K. Eswaraiah, "Optimization of EDM Process parameters in Machining of 17-4 PH Steel using Taguchi Method," *Materials Today: Proceedings*, vol. 4, no. 2, pp. 2040-2047, 2017.
[27] O. O. Agboola *et al.*, "Optimization of heat treatment parameters of medium carbon steel quenched in different media using Taguchi method and grey relational analysis," *Heliyon*, vol. 6, no. 7, p. e04444, Jul 2020.
[28] R. Ramadass, S. Sambasivam, and K. Thangavelu, "Selection of optimal parameters in V-bending of Ti-Grade 2 sheet to minimize springback," *Journal of the Brazilian Society of Mechanical Sciences and Engineering*, vol. 41, no. 1, pp. 1-11, 2019.
[29] N. Tamilselvan, M. Thirumarimurugan, and E. Sudalai Manikandan, "Study on various control strategies of plate type heat exchanger for non-Newtonian fluids," *Journal of Ambient Intelligence and Humanized Computing*, vol. 12, no. 7, pp. 7253-7261, 2021.
[30] A. G. Thakur, T. E. Rao, M. S. Mukhedkar, and V. M. Nanedkar, "Application of Taguchi Method for Resistance Spot Welding of Galvanized Steel," vol. 5, no. 11, 2010.
[31] A. D. Shieddieque, S. Sukarman, M. Mardiyati, B. Widyanto, and Y. Aminanda, "Multi-objective Optimization of Sansevieria Trifasciata Fibre Reinforced Vinyl Ester (STF/VE) Bio-composites for the Sustainable Automotive Industry," *Automotive Experiences*, vol. 5, no. 3, pp. 288-303, 2022.
[32] A. Budianto, S. Sukarman, S. B. Jumawan, and A. Abdulah, "OPTIMASI RESPON TUNGGAL PADA PROSES TEXTURING BENANG DTY-150D / 96F MENGGUNAKAN METODE TAGUCHI SINGLE RESPONSE OPTIMIZATION OF DTY-150D / 96F YARN TEXTURING PROCESS USING TAGUCHI METHOD," *Arena Tekstil*, vol. 35, no. 2, pp. 77-86, 2020.
[33] A. Badrish, A. Morchhale, N. Kotkunde, and S. K. Singh, "Parameter Optimization in the Thermo-mechanical V-Bending Process to Minimize Springback of Inconel 625 Alloy," *Arabian Journal for Science and Engineering*, vol. 45, no. 7, pp. 5295-5309, 2020.
[34] S. Sukarman, A. D. Shieddieque, C. Anwar, N. Rahdiana, and A. I. Ramadhan, "Optimization of Powder Coating Process Parameters in Mild Steel (Spcc-Sd) To Improve Dry Film Thickness," *Journal of Applied Engineering Science*, vol. 19, no. 2, pp. 1-9, 2021.
[35] Minitab. (2023, 10/12/2023). *Overview for Probability Plot*.
[36] A. Abdelkefi, M. R. Hajj, and A. H. Nayfeh, "Power harvesting from transverse galloping of square cylinder," *Nonlinear Dynamics*, vol. 70, no. 2, pp. 1355-1363, 2012.